A. Bakker and R. W. J. Koers†*

Prediction of Cleavage Fracture Events in the Brittle–Ductile Transition Region of a Ferritic Steel

REFERENCE Bakker, A. and Koers, R. W. J., **Prediction of cleavage fracture events in the brittle–ductile transition region of a ferritic steel**, *Defect Assessment in Components – Fundamentals and Applications*, ESIS/EGF9 (Edited by J. G. Blauel and K.-H. Schwalbe) 1991, Mechanical Engineering Publications, London, pp. 613–632.

ABSTRACT Two- and three-parameter Weibull probability distributions of the cleavage fracture stress were determined from experiments and finite element computations on round notched tensile specimens. These distributions were used to predict the cleavage fracture behaviour of cracked three-point and four-point bend specimens, and of a wide plate with a central hole with edge cracks. Experimental results are found to fall within the predicted 90 percent cleavage fracture ranges predicted for these geometries. The differences between predictions based on the two- and three-parameter Weibull distributions are small compared to the predicted 90 percent ranges. However, at low probability values which are of interest for the failure assessment of structures with unacceptable failure impact, the two models differ significantly. With the two-parameter distribution a continuously dropping critical failure load for decreasing failure probability is predicted. Application of the three-parameter distribution results in the prediction of a threshold value of the critical failure load which is more realistic. Together with the observation that the threshold value of the J integral at cleavage fracture is almost geometry-independent; this makes the three-parameter Weibull model a potentially powerful tool for cleavage fracture assessments.

Introduction

Within the first phase of the NIL (Netherlands Welding Institute) International Collaborative Fracture Programme (1), various cracked geometries of a ferritic structural steel were tested in the brittle–ductile transition temperature region, and analysed by common safety assessment methods based on the critical crack opening displacement (CTOD) and the critical J integral. The accuracy of such predictions is limited by the large scatter of these critical, single parameter fracture mechanics parameters in this temperature region.

The large scatter of critical fracture parameters suggests that a statistical approach should be used for the prediction of cleavage fracture probabilities of cracked structures operating in the transition temperature region (2)(3). The present paper describes the application of a 'local approach' model based on two- and three-parameter Weibull distributions (4) of the maximum normal stress at cleavage fracture. These models are applied to some of the geometries tested within the first phase of the NIL fracture programme.

* Delft University of Technology, Laboratory for Materials Science, P.O. Box 5025, 2600 GA Delft, The Netherlands.
† Shell Research B.V., P.O. Box 40, 6800 AA Arnhem, The Netherlands.

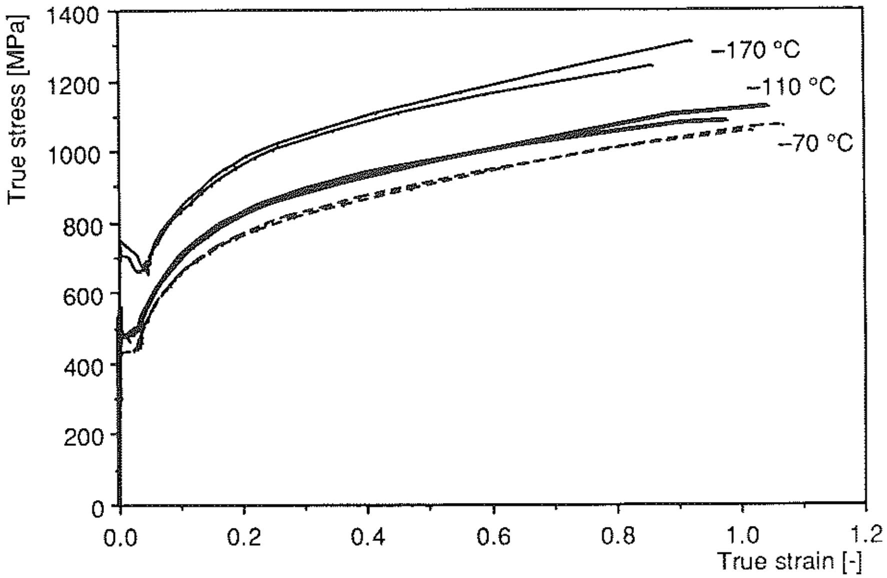

Fig 1 Material true stress–strain curves at −70, −110, and −170°C

Material

The material applied in this study is a ferritic C–Mn steel with designation Fe510Nb of quality Fe 355-KT according to Euronorm 113-72. This material has been investigated extensively within the NIL fracture programme **(1)**. Typical true-stress versus true-strain curves measured on smooth round tensile specimens at the temperatures −70°C, −110°C and −170°C, corresponding to the temperatures of the fracture mechanics tests to be applied, are shown in Fig. 1. During the tensile tests the true strain was measured by monitoring the diameter contraction at the necking region. True stress computations were based on this measurement and were corrected for the tri-axial stress state in the necking region according to the procedure proposed by Bridgeman **(5)**.

Experiments and computations on notched specimens

Two series of 18 round tensile specimens with a circumferential 'V' notch according to Fig. 2 were fractured at temperatures of −110°C and −170°C respectively. During the experiments the diameter contraction at the root of the notch was recorded with a special clip-gauge. The variation of the measured contraction of diameter at fracture for both series is shown in Fig. 3. All fractures at both temperatures occurred beyond net section yielding. Microscopic observation of the fracture surfaces showed clearly that at −170°C the complete fractures were by cleavage. At −110°C the fractures were also by cleavage, but at the notch-root small areas (≈ 0.2 mm) showed a ductile fracture appearance.

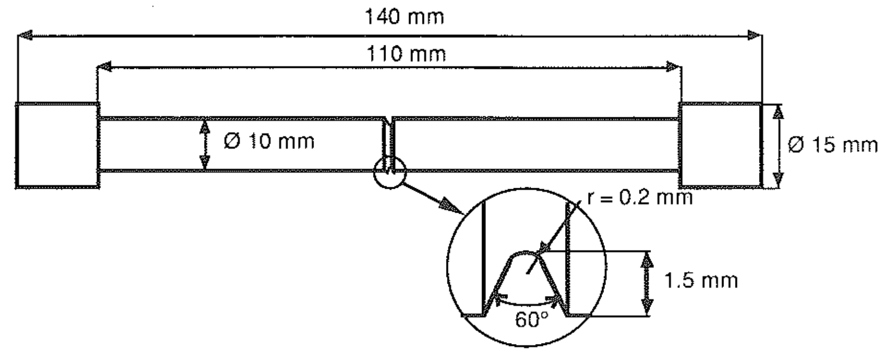

Fig 2 Geometry of notched tensile specimens

Finite element analyses of the tensile specimens were performed for both experimental temperatures with the MARC general purpose finite element system (version K3). Large strain and displacement effects were included in these analyses by applying an updated Lagrange procedure in order to obtain the best possible estimates for the stress distributions near the notch root, where strains may grow in excess of 100 percent. Four-node quadrangular axi-symmetric elements were applied, as initial attempts to use 8-node elements failed through excessive warping of elements by large displacements. The mesh contained 853 nodal points and 792 elements. Figure 3 shows the calculated net-section axial stress (axial load/undeformed cross-sectional area)

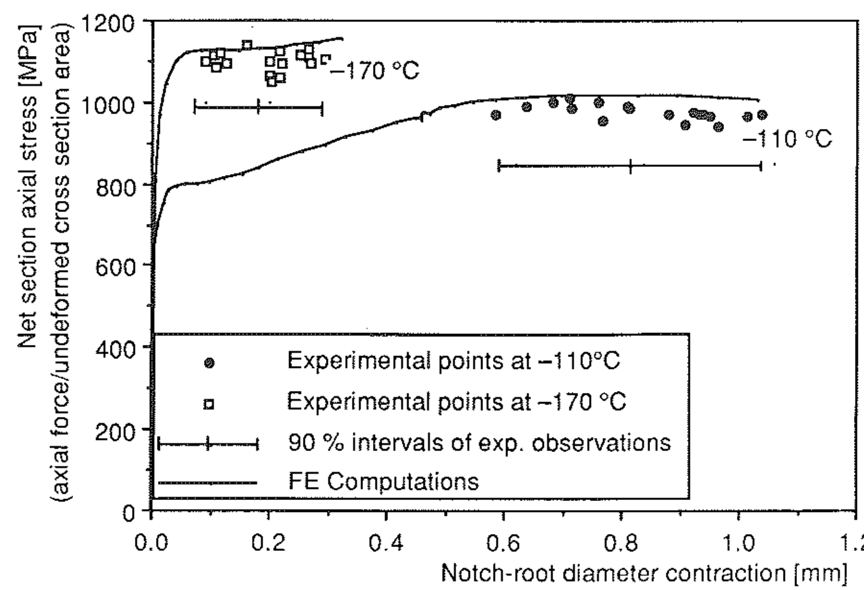

Fig 3 Variance of the experimentally observed notch-root diameter contraction of the notched tensile specimens at fracture

versus notch-root diameter contraction compared with the experimental points at fracture. At both test temperatures the calculated net-section stress is in the upper region of the experimental scatter. The most plausible reason for this is that the yield stress used in the analyses was somewhat higher than the

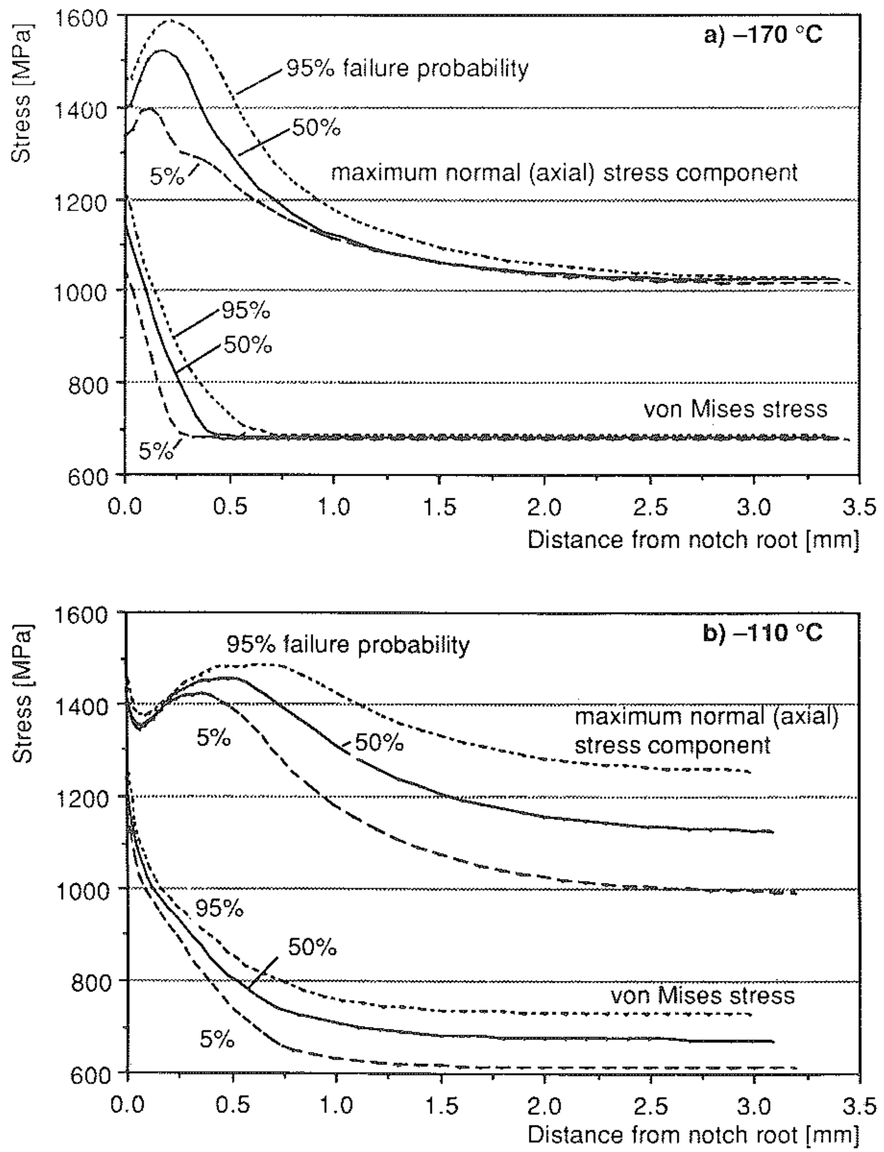

Fig 4 Calculated maximum normal stress and von Mises equivalent stress across the net section of the notched tensile specimens at the mean and extremes of the 90 percent confidence interval of the notch–root diameter contraction at fracture: (a) Temperature −170°C; (b) Temperature −110°C

actual mean value. The observed variation of the (upper and lower) yield stress was relatively high. However, it is not expected that this has much effect on the results to be used for this investigation, since the stress–strain levels of interest are well beyond yielding, i.e., in the strain-hardening region which shows far less variation than the yield stress.

Figure 4 shows the calculated maximum normal stress (corresponding with the axial stress component) and the von Mises equivalent stress at the mean and the extremes of the 90 percent confidence limits of the experimentally observed diameter contraction at the notch-root indicated in Fig. 3.

Cleavage fracture probability distributions

The variation of the contractions of the diameter (*cf.* Fig. 3) and stress distributions (*cf.* Fig. 4) at fracture requires a statistical approach. The stress distributions of Fig. 4 indicate that fractures at −170°C occur at higher values of the maximum normal stress, but that the highly stressed volume ahead of the notch–root is larger at −110°C. So the maximum normal stress at cleavage fracture decreases for increasing stressed volume. This points towards a weakest link approach, which incorporates volume effects in the fracture prediction, as for instance proposed by Wallin, Saario, and Törrönen **(2)** and Beremin **(3)** and previously recommended within the framework of this study **(6)(7)**.

Two-parameter Weibull model

In the first instance a two-parameter Weibull weakest link model was applied. It is assumed that the cleavage probability, P_F, of a reference volume V_0 stressed by a maximum normal stress σ is given by a two-parameter Weibull distribution **(4)**

$$P_F = 1 - \exp\left\{-\left(\frac{\sigma}{\sigma_u}\right)^m\right\} \text{ for } \varepsilon_{pl} > 0, \text{ and } P_F = 0 \text{ for } \varepsilon_{pl} = 0 \qquad (1)$$

where m is the Weibull parameter, σ_u is the characteristic (63 percent value) of the distribution, and ε_{pl} is plastic strain. The distribution is cut off at a maximum normal stress equal to the material yield stress, since cleavage fracture must always be preceded by some amount of plastic deformation. For a structure with volume V stressed by a non-uniform maximum normal stress distribution $\sigma(x)$, the weakest link assumption leads to a failure probability according to:

$$P_F = 1 - \exp\left\{-\int_{V_{ys}} \left(\frac{\sigma(x)}{\sigma_u}\right)^m \frac{dV}{V_0}\right\} \qquad (2)$$

where V_{ys} is the part of volume V with plastic strain $\varepsilon_{pl} > 0$. Note that σ in equation (1) and $\sigma(x)$ in equation (2) must be taken as the *maximum normal* *stress that the material point has experienced during its entire loading history.* Although only monotonically increasing loading situations were considered in these investigations, local unloadings do occur near notch and crack tips. The point with maximum normal stress moves away from the notch or crack tip with increased loading, which causes partial unloading at points between the tip and the highest stressed point. If this loading history effect is not taken into consideration, the cleavage probability could decrease with increased loading, which is physically impossible.

By defining the 'Weibull stress' of the stress distribution within the structure according to

$$\sigma_W = \left\{ \int\!\!\int_{V_{ys}} \sigma(x)^m \frac{dV}{V_0} \right\}^{1/m} \tag{3}$$

equation (2) may be written as

$$P_F = 1 - \exp\left\{ -\left(\frac{\sigma_W}{\sigma_u} \right)^m \right\} \tag{4}$$

which is identical to the distribution for the reference volume according to equation (1) for a maximum normal stress equal to the structure's Weibull stress.

The Weibull parameter m may be determined by an iterative process. Assuming values for m and the reference volume V_0, the Weibull stress at the experimentally observed fracture points is computed from the finite element results with equation (3). A linear regression of $\ln[\ln\{1/(1-P_F)\}]$ versus $\ln(\sigma_W)$, with P_F values at the fracture points taken equal to the rank probability of the fracture points within the series, then results in a slope m^* and a σ_u value. This is repeated with an adjusted m value for computing the Weibull stress until the regression slope m^* is equal to the assumed m value. Note that the choice of the reference volume V_0 does not play a role in this convergence process and does not affect the Weibull parameter m. It affects the values of the Weibull stresses such that the Weibull stress σ_W^* for a reference volume V_0^* is related to the Weibull stress σ_W calculated for a reference volume V_0 according to

$$\sigma_W^* = \left\{ \int\!\!\int_{V_{ys}} \sigma(x)^m \frac{dV}{V_0^*} \right\}^{1/m} = \left(\frac{V_0}{V_0^*} \right)^{1/m} \sigma_W \tag{5}$$

The constant ratio between Weibull stresses for different reference volumes causes a constant shift of the $\ln(\sigma_W)$ points in a $\ln[\ln\{1/(1-P_F)\}]$ versus $\ln(\sigma_W)$ plot, and hence does not change the m value (slope) of the regression. Only the characteristic value σ_u changes to σ_u^*, in exactly the same way as the Weibull stresses according to equation (5).

Figure 5 shows the result of the iteration process described above. For $-170°C$ convergence is reached for $m = 25.4$. However, for $-110°C$ convergence could not be achieved. This is possibly caused by the fact that at $-110°C$ some ductile tearing preceded the cleavage fracture, which was not accounted for by the finite element computations. No other explanation could be found for this behaviour. The probability distribution for the converged m value of 25.4 is compared with the fracture points in Fig. 6. The reference volume V_0 was taken equal 1 mm^3. No physical interpretation is given to this, since it was already observed that V_0 only serves as a scaling parameter for the Weibull distribution which has no effect on the final probability result. Figure 6 also shows the fracture points at $-110°C$ computed with the converged m value of 25.4 for $-170°C$. These clearly deviate from the $-170°C$ distribution. If this deviating behaviour is not caused by ductile tearing preceding cleavage fracture, this would mean that the cleavage fracture probability distribution is not temperature-independent and by that not suitable for predicting cleavage stress events at other temperatures. This aspect will be further discussed when cleavage predictions of fracture specimens are dealt with.

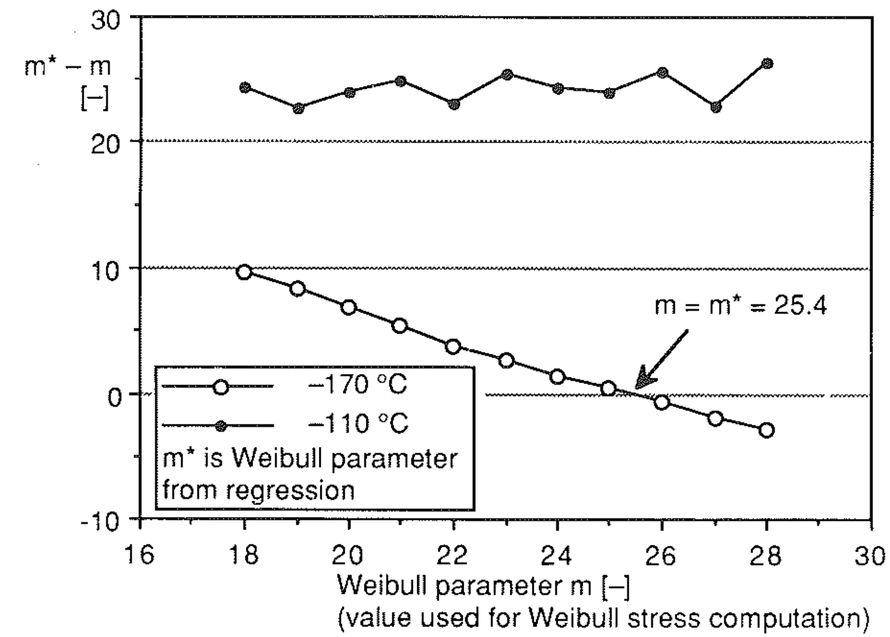

Fig 5 Iteration process for the determination of the Weibull parameter *m*

Three-parameter Weibull model

In the two-parameter Weibull model described above, a point in the material contributes to the cleavage probability as soon as plasticity occurs. Whether this is true in reality is doubtful. The yield stress in the temperature region -70 to $-170°C$ varies between ≈ 440 MPa and ≈ 700 MPa (*cf.* Fig. 1).

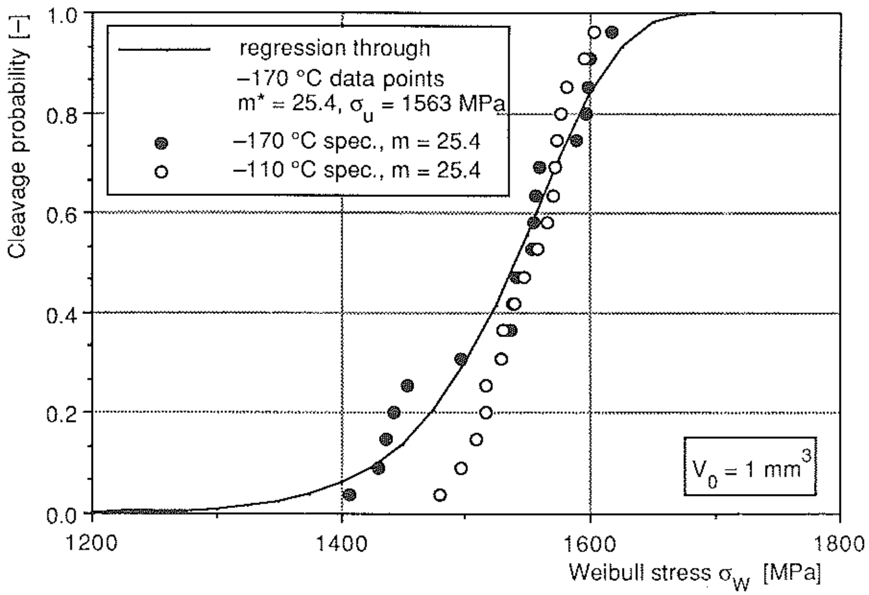

Fig 6 Two-parameter Weibull distribution of cleavage fracture stress determined on notched tensile specimens

However, at 20°C, which is in the upper shelf region, tensile specimens always fail by a ductile (cup and cone) mechanism at appreciably higher stresses than these yield levels at low temperature. This indicates that there is some threshold value for the maximum normal stress below which cleavage fracture cannot be triggered and which is considerably higher than the yield stress. In the three-parameter Weibull model the cleavage probability, P_F, of a characteristic volume V_0 stressed by a maximum normal stress σ is given by

$$P_F = 1 - \exp\left\{-\left(\frac{\sigma - \sigma_{th}}{\sigma_u - \sigma_{th}}\right)^m\right\} \text{ for } \sigma \geqslant \sigma_{th} \quad \text{and} \quad P_F = 0 \text{ for } \sigma < \sigma_{th} \tag{6}$$

where m is the Weibull parameter, σ_u is the characteristic (63 percent value) of the distribution, and σ_{th} is the threshold stress below which cleavage cannot be triggered. For a structure with volume V stressed by a non-uniform maximum normal stress distribution $\sigma(x)$ the weakest link assumption then leads to a failure probability according to

$$P_F = 1 - \exp\left\{-\int_{V_{th}}\left(\frac{\sigma(x) - \sigma_{th}}{\sigma_u - \sigma_{th}}\right)^m \frac{dV}{V_0}\right\} \tag{7}$$

where V_{th} is the part of the volume V with maximum normal stress $\sigma(x) > \sigma_{th}$. As for the two-parameter Weibull model, σ in equation (6) and $\sigma(x)$ in equation (7) must be taken as the maximum normal stress experienced at a point in

the material during the loading history in order to account for local unloading effects.

By defining the 'Weibull stress' of the stress distribution within the structure according to

$$\sigma_W = \sigma_{th} + \left\{\int_{V_{th}} (\sigma(x) - \sigma_{th})^m \frac{dV}{V_0}\right\}^{1/m} \tag{8}$$

equation (7) may be written as

$$P_F = 1 - \exp\left\{-\left(\frac{\sigma_W - \sigma_{th}}{\sigma_u - \sigma_{th}}\right)^m\right\} \text{ for } \sigma_W \geqslant \sigma_{th}, \quad \text{and} \quad P_F = 0 \text{ for } \sigma_W < \sigma_{th} \tag{9}$$

which is identical to the distribution for the reference volume according to equation (6), for a maximum normal stress equal to the structure's Weibull stress.

When a threshold value is assumed, the determination of the Weibull parameter m can be determined in exactly the same way as for the two-parameter model. As for the two-parameter model, the choice of V_0 does not play a role in this. Figure 7 shows the results for the converged m value at −170°C. For −110°C the process did again not converge. Figure 7 shows the regression m value at −110°C when the converged m value at −170°C is used

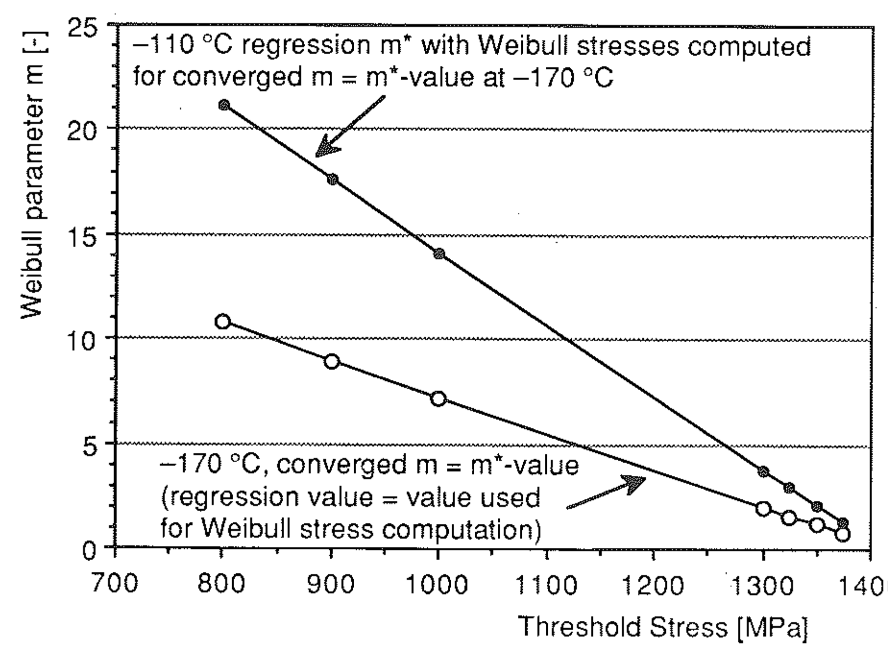

Fig 7 Weibull parameter m as a function of threshold stress level

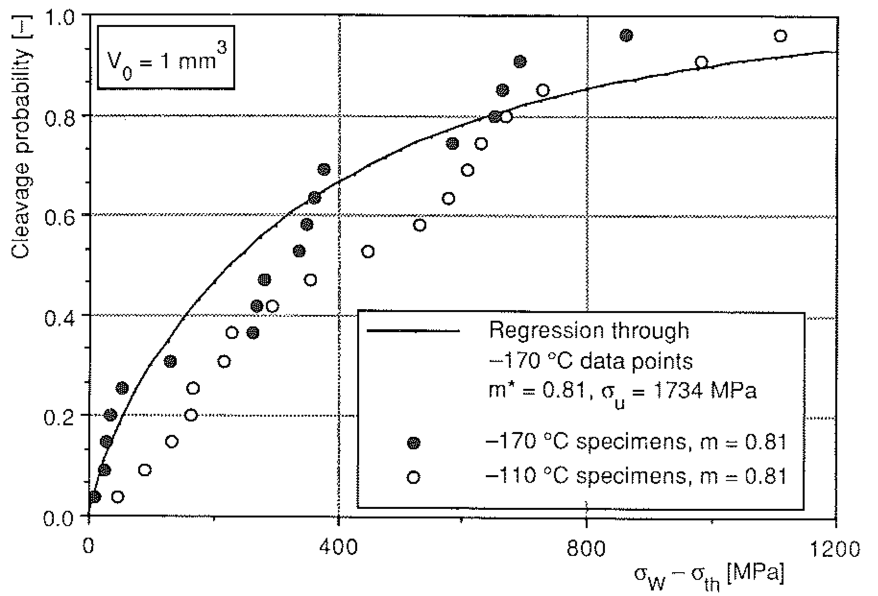

Fig 8 Three-parameter Weibull distribution of cleavage fracture stress determined on notched tensile specimens

for the Weibull stress computation. For increasing threshold stress these results seem to approach each other, suggesting convergence at a threshold stress just above 1400 MPa. However, the actual threshold stress cannot be that high, since the lowest maximum normal stress level at which a specimen failed is also just above 1400 MPa. Bearing in mind the results of the tensile tests discussed above, it was decided to use a high value for the threshold stress equal to 1375 MPa for the failure predictions to be discussed later. The probability distribution for the converged m value of 0.81 at −170°C is compared with the fracture points in Fig. 8. The reference volume V_0 was taken as 1 mm³ in this case. This figure also shows the fracture points at −110°C computed with the same m value. The fracture points at −110°C still deviate from the −170°C distribution, but lie considerably closer to it than for the two-parameter model shown in Fig. 6. This result suggests a temperature-independent probability distribution for cleavage stress which is required for predicting the behaviour at other temperature levels. The small deviation could be caused by the ductile tearing preceding final fracture at −110°C.

Fracture predictions

The two- and three-parameter Weibull stress distributions of the cleavage fracture stress were used to predict the behaviour of fracture mechanics test specimens of the same material which had been fractured experimentally **(1)**. These were:

- single edge notched specimens tested in three-point bending (3PB), with width $W = 60$ mm, relative crack depth $a/W = 0.5$, and thickness $B = 30$ mm;
- single edge notched specimens tested in four-point bending (4PB), with width $W = 30$ mm, relative crack depth $a/W = 0.3$, and thickness $B = 30$ mm, 70 mm, and 110 mm;
- wide plates with a central hole with edge cracks (WP), *cf.* Fig. 9.

Although experiments on these specimens were performed at different temperatures (−20, −40, and −70°C), the predictions to be discussed here will be limited to −70°C since at higher temperatures the amount of stable crack growth preceding cleavage fracture was too large to be neglected. At −70°C the amount of stable crack growth was almost always smaller than 0.2 mm. It was verified by a finite element analysis that up to this level of stable crack growth the effects on the near tip stresses are only marginal.

Two-dimensional finite element analyses were performed for all three geometries described above, applying an updated Lagrange description in order to account for large strain/large displacement effects. Plane strain,

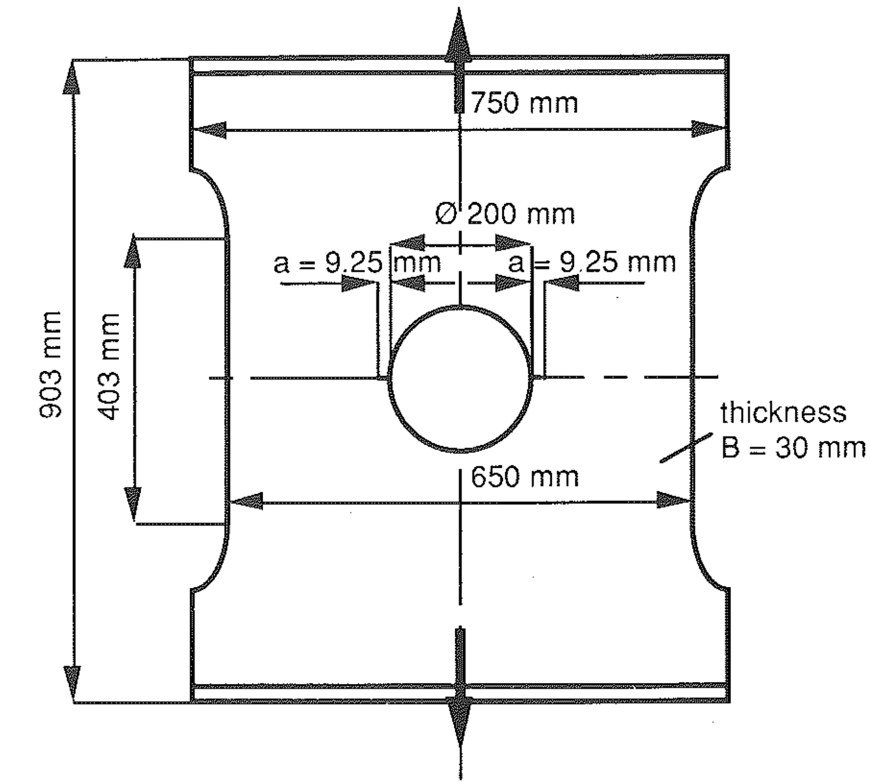

Fig 9 Wide plate test specimens used for cleavage predictions

4-node (bi-linear) elements were applied, as for these analyses too it was experienced that quadratic elements showed excessive warping at large deformations. The crack tip was modelled by a small circle with a radius of 0.01 mm in order to avoid the need to use singular elements at the start of the computation. The use of a plane strain assumption is only correct in the close vicinity of the crack tip. However, the material volume that contributes to the cleavage probability is also limited to a small region around the crack tip, which is actually in plain strain. Although for the two-parameter Weibull model the entire plastic zone contributes to the Weibull stress and thus to the cleavage probability, the high value of the *m* parameter means that only the highest stressed points near the crack tip will in the model contribute towards the fracture probability. In the future three-dimensional analyses will have to show to what extent the predictions are influenced by the plane strain assumption, but within the limitations of a two-dimensional analyses plane strain is the best possible approximation of the stress state. In spite of ever increasing computer power, three-dimensional large deformations/large displacement analyses, which are required for this purpose in order to obtain a good approximation of the near-tip stress/strain field, are still extremely expensive.

Predicted geometry effects

From the calculated element stresses the Weibull stresses as a function of applied loading for the two- and three-parameter Weibull model were calculated from, respectively, equations (3) and (8) with a post-processing program and using m, V_0, and σ_u values as indicated in Figs 6 and 8. During the analysis the J integral was calculated using the MARC J integral option. The J integral was chosen as the single fracture parameter to compare the results for different geometries because this parameter is better defined and has a more sound theoretical basis than the crack-tip opening displacement (CTOD). However, when a consistent definition of CTOD is used, the forthcoming observations could also be made for this parameter. From the Weibull stresses as a function of applied loading the failure probability as a function of applied loading was calculated from equation (4) for the two-parameter Weibull model and from equation (9) for the three-parameter model.

Figure 10 shows the resulting cleavage fracture probability for all geometries with a thickness B = 30 mm as a function of the J integral. Note that for the wide plate (WP) specimens two predictions were made. The first ('1 tip') prediction follows from the Weibull stress computation for one crack tip only. It has no real physical meaning because in reality this specimen always has two crack tips, but the result compared with that for the bend specimens shows how the difference in stress state between a tension geometry and a bending geometry affects the cleavage probability. The in-plane constraint ahead of the crack tip of a tension geometry is lower than that for a bending geometry. This results in lower maximum normal stresses at the same defor-

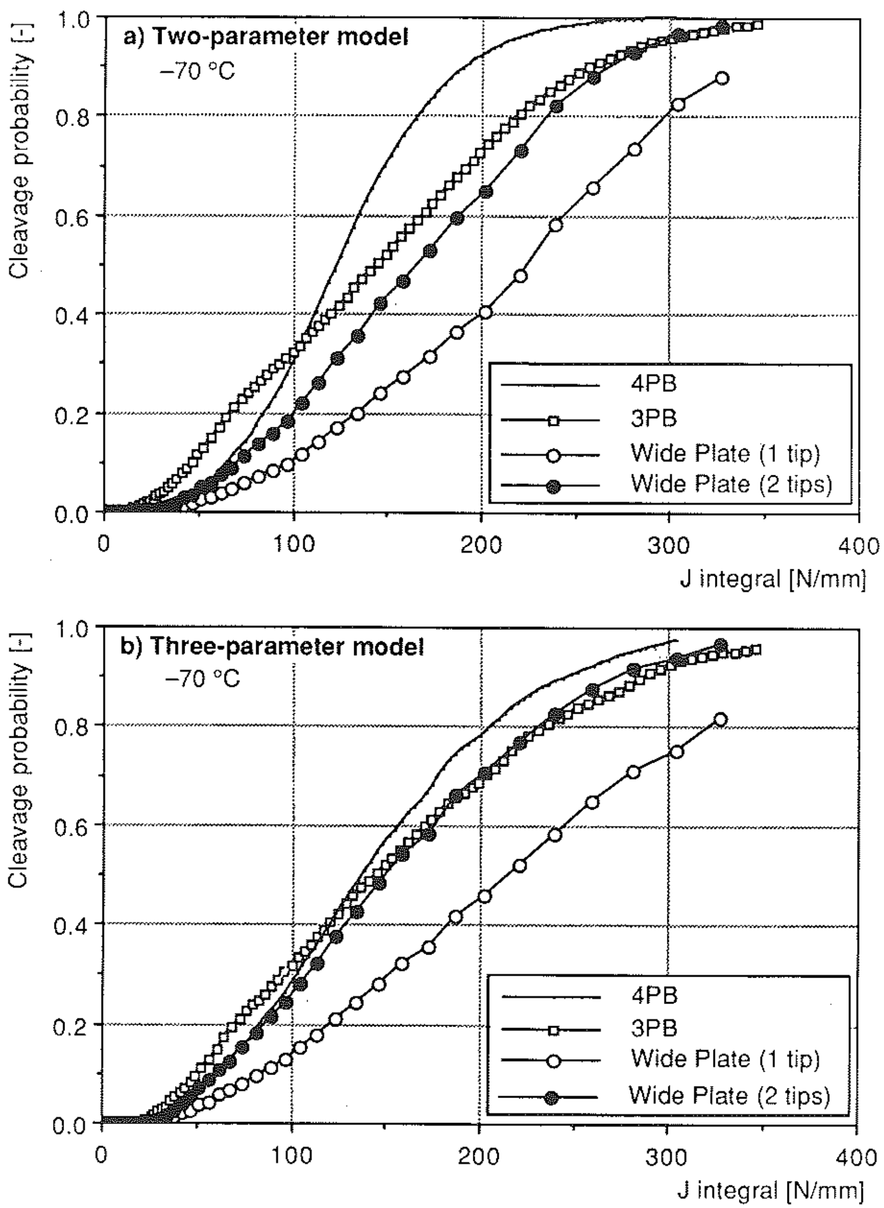

Fig 10 Predicted cleavage fracture probability at −70°C for the three specimen types: (a) Two-parameter Weibull model (*cf.* Fig. 6); (b) Three-parameter Weibull model (*cf.* Fig. 8)

mation levels and leads consequently to lower Weibull stresses and cleavage probabilities for tension geometries. Figure 10 clearly shows that this effect is cancelled when the cleavage probability for the complete specimen ('2 tips') is determined by computing the Weibull stresses for the complete geometry, i.e., by doubling the volume integral for one crack tip. The cleavage probability distribution for the complete wide plate closely approaches that of the 3PB specimens. This indicates that when the experimentally observed cleavage behaviour of wide plate specimens is in good agreement with that of bend specimens, this is no proof that the stress state in these specimens is similar. The lower constraint in the wide plates is simply compensated by the doubling of the process volume in the vicinity of the crack that contributes to the cleavage probability. This single result does not prove that this will always be the case. Different geometries will have to be evaluated in a similar way to verify this. However, this example does illustrate that the cleavage probability is very sensitive to the number of possible cleavage triggering points (crack tips) in a geometry.

The differences between the three geometries and between the two- and three-parameter models are relatively small. An exception is the 4PB specimen for the two-parameter model, which predicts a lower variation of the J integral at cleavage fracture compared to the other geometries. For the three-parameter model this effect is far less pronounced. Further detailed study of the calculated stress distributions is required to explain this behaviour.

In order to enable a comparison with experimental results, the predicted 90 percent cleavage probability ranges which follow from Fig. 10 are plotted in Fig. 11 together with the experimental points. The experimental J values for the bending geometries were determined from the area under the load versus load-line displacement curves, as is used for standard J measurements. For the wide plate geometry no such J solution is available, and the computed J value at the experimentally observed cleavage load was used instead. Some experiments showed an amount of ductile tearing prior to cleavage fracture larger than 0.2 mm. These points are indicated separately, since it is expected that the present finite element analyses are not valid for this situation. This would require analyses accounting for crack growth. Two effects will oppose each other: the growth of the maximum stresses is slowed down by the tearing process but the sampling volume for cleavage nuclei increases by the crack tip movement. Without the results of crack growth computation it is difficult to foresee what the combined effect will be. Figure 11 contains three such points, two for the 4PB specimens and one for the 3PB specimens. That for the 3PB specimen is high in the predicted 90 percent cleavage probability range, those for the 4PB specimens are above it. Together with the observation that all experimental points with no or very little (<0.2 mm) ductile tearing fall within the predicted 90 percent cleavage probability ranges, this leads to the conclusion that ductile tearing has a shielding effect, i.e. that it slows down the increase of the Weibull stress with increasing load.

Predicted thickness effects

As the 4PB specimens were tested in three thicknesses (30, 70, and 110 mm), the thickness effect on cleavage fracture behaviour could also be studied.

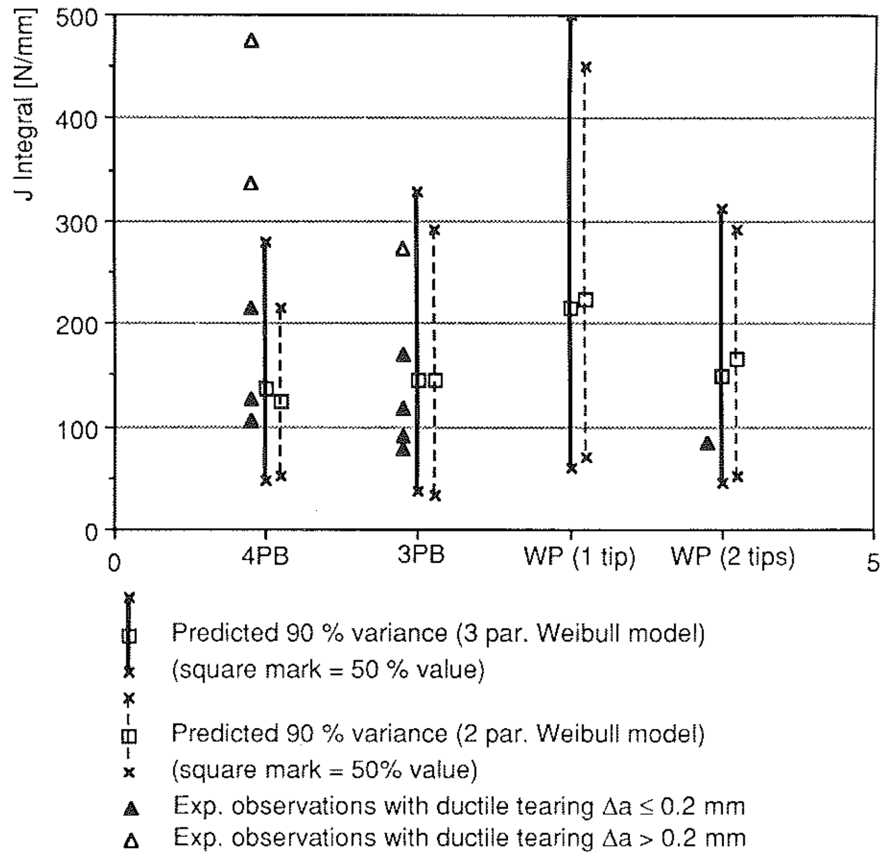

Fig 11 Predicted 90 percent cleavage fracture ranges at −70°C for the three specimen types with thickness B = 30 mm compared with experimental observations

Figure 12 shows the predicted cleavage fracture probability in terms of the applied J integral for these three thicknesses. Both models clearly predict a thickness effect, resulting in a decreasing mean value of J at cleavage fracture and a decreasing variation with increasing thickness, as can be expected from a weakest link assumption. The two-parameter model predicts smaller ranges, but equivalent mean values. The thickness effect and the comparison between the two models also follows from Fig. 13, which compares the predicted 90 percent cleavage probability ranges for the three thicknesses, and also shows the experimental observations. All experimental points fall within the predicted 90 percent ranges, except for the two points with ductile tearing Δa larger than 0.2 mm (the same points as in Fig. 11).

Choice between two- and three-parameter Weibull models

The number of experimental points in Figs 11 and 13 is too low and the differences between the 90 percent cleavage probability ranges of the two- and

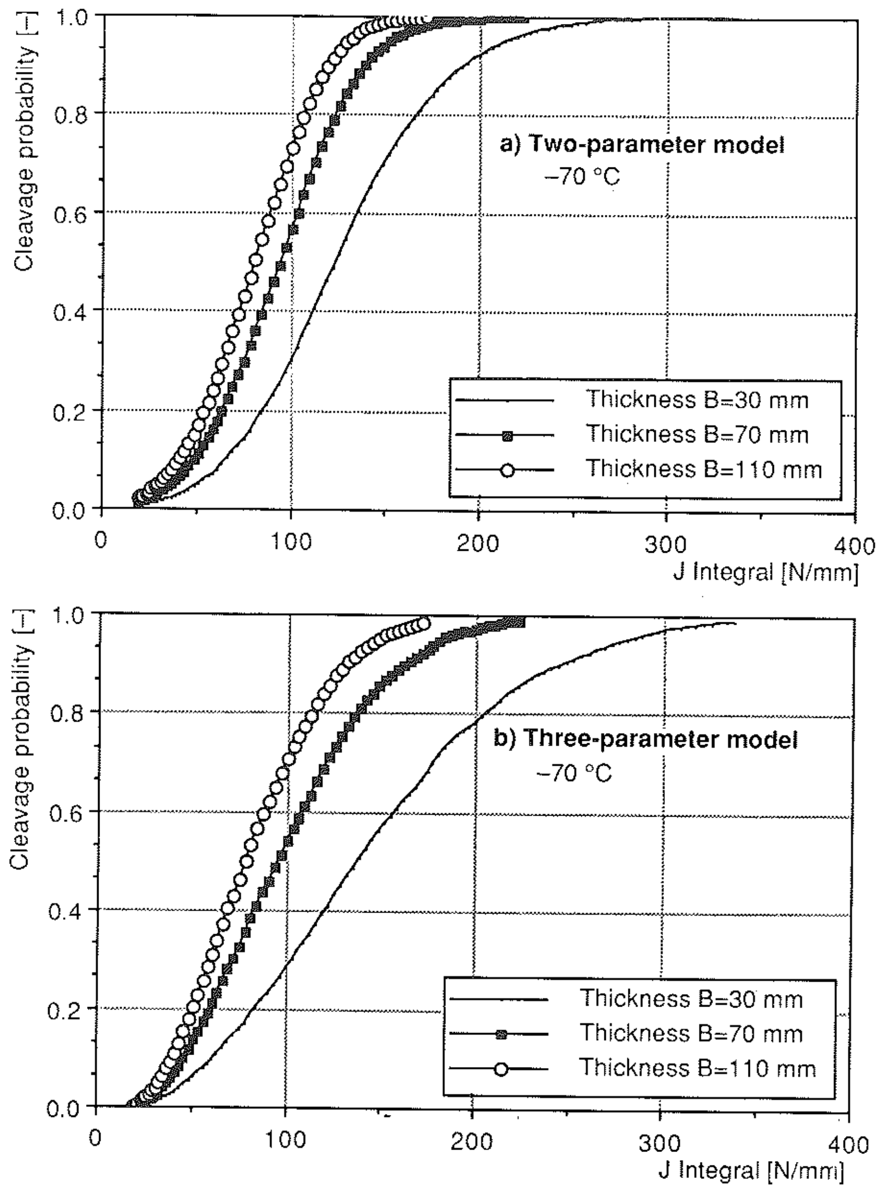

Fig 12 **Predicted cleavage fracture probability at −70°C for four-point bend specimens with thickness equal to 30, 70, and 110 mm: (a) Two-parameter Weibull model (*cf.* Fig. 6); (b) Three-parameter Weibull model (*cf.* Fig. 8)**

three-parameter Weibull models too small to give any indication as to which of these models is the better. On the basis of these results one could argue that the differences between the two models are so small that the simplest one, i.e., the two-parameter model, is to be preferred. What still needs to be clarified is

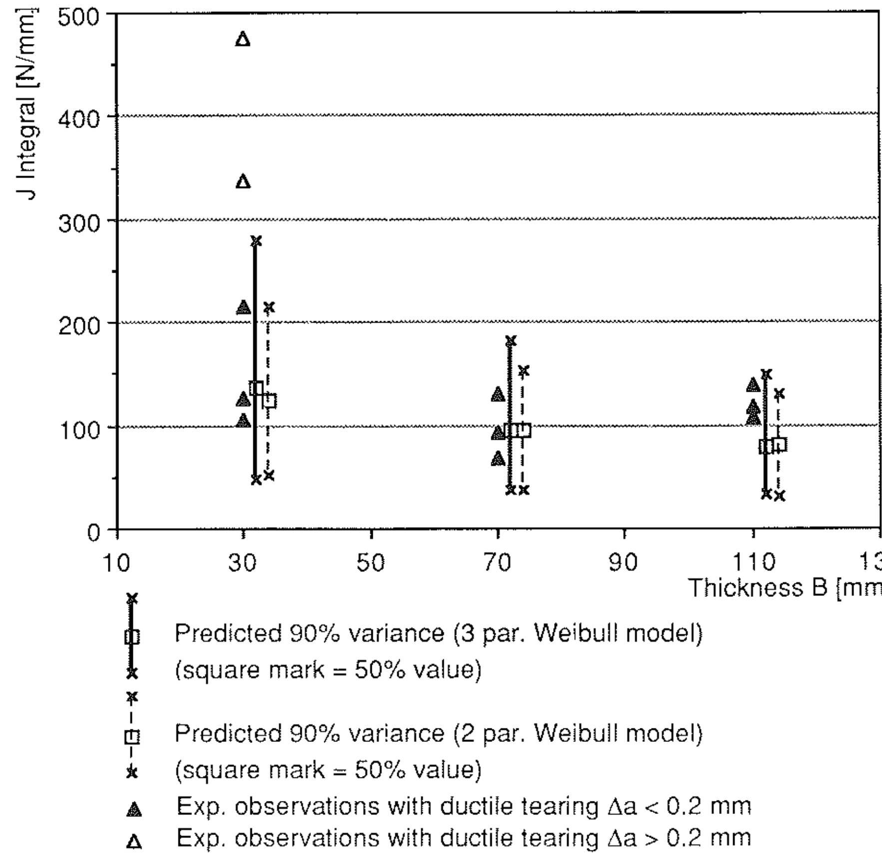

Fig 13 **Predicted 90 percent cleavage fracture ranges at −70°C for four-point bend specimens with thickness equal to 30, 70, and 110 mm**

the reason why the cleavage probability distributions determined on the notched tensile specimens for the two-parameter model differ considerably for the two temperatures −170 and −110°C. The present predictions for −70°C are based on the distributions for −170°C, and seem to work well, in spite of the previous discrepancy. A possible explanation is the small amount of ductile tearing of the notched specimens tested at −110°C. The large Weibull parameter, $m = 25.4$, for the two-parameter model means that Weibull stresses become very sensitive to small differences in stress levels. The results for the three-parameter model with $m = 0.81$ are far less sensitive, which could explain why the differences in cleavage probability distributions for the notched specimens tested at −170°C and −110°C are much smaller than for the two-parameter model.

Another aspect in the choice between the two models is the prediction at low probability values. For structures which must have a high reliability because failure has unacceptable consequences for people and/or environment (nuclear installations, chemical plants, off-shore structures) failure probabilities must be limited to extremely low values (10^{-4}–10^{-6}). That can only be realised when also the material behaviour is known for such low probability values. Figure 14 shows a blow-up of Fig. 10 at low probability values. The two models appear to give almost identical results for cleavage probabilities larger than about 10^{-2}. Below this level the models start to deviate considerably. The two-parameter model always predicts a finite probability of failure whereas no failure is possible with the three-parameter model below a threshold value. The load level at which this occurs is dependent of the size of the element mesh applied at the crack tip and has no relation to actual material behaviour. However, the three-parameter model predicts some threshold value for J_c at cleavage. Because of the finite load steps used in the finite element analyses, the precise value of this threshold for J_c cannot be given. It lies between the last load step for which the cleavage probability is zero and the next step with non-zero probability. For the three test specimens these figures are:

3PB	$J = 18.2$ N/mm, $P_F = 0$	$J = 19.8$, $P_F = 2 \times 10^{-3}$
4PB	$J = 19.8$ N/mm, $P_F = 0$	$J = 20.9$, $P_F = 2 \times 10^{-4}$
WP–1 tip	$J = 21.5$ N/mm, $P_F = 0$	$J = 24.4$, $P_F = 1 \times 10^{-3}$
WP–2 tips	$J = 21.5$ N/mm, $P_F = 0$	$J = 24.4$, $P_F = 2 \times 10^{-3}$

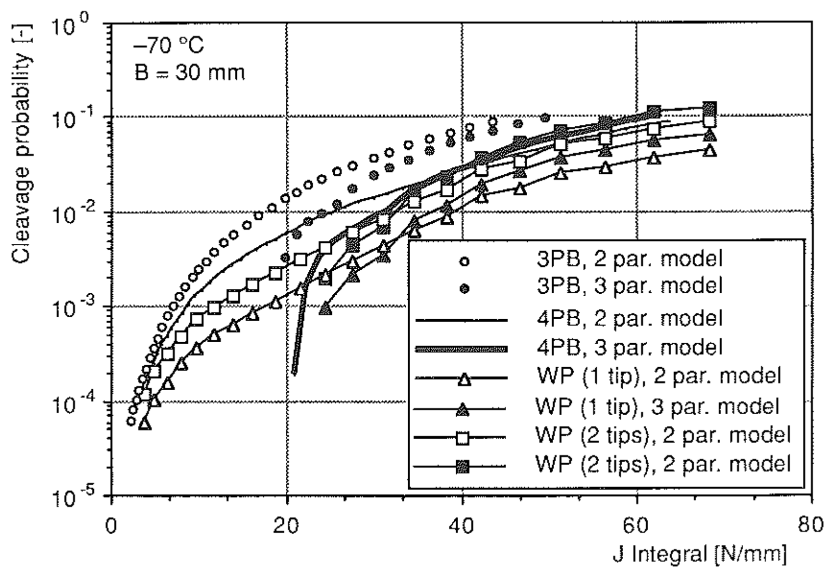

Fig 14 Comparison of the cleavage probability of the 3PB, 4PB, and WP specimens with thickness B = 30 mm at −70°C at low probability levels as predicted by the two- and three-parameter models

Omitting the (fictitious) '1 tip' WP solution and taking the lowest figures for $P_F = 0$, this results in a mean value for $J_c = 19.8$ N/mm ± 8 percent.

Note that for the threshold behaviour the differences between the '1 tip' and '2 tips' predictions vanish. This means that with a threshold J_c value for cleavage based on three-parameter Weibull distribution for the cleavage fracture stress, a deterministic failure assessment may be performed for the largest defect (crack) in a structure. The three-parameter model therefore seems to have more potential for the assessment of components which must have an extremely low failure probability.

Conclusions and recommendations

- Predictions were made of the cleavage fracture behaviour of cracked three-point bend (3PB), four-point bend (4PB), and wide plate (WP) geometries with a central hole with edge cracks, based on two- and three-parameter Weibull probability distributions of the cleavage fracture stress measured on notched round tensile specimens. The predictions of both models are in good agreement with experimental results, both with respect to the prediction of geometry effects and thickness effects.
- The cleavage probability predictions for the wide plate geometries suggest that this geometry has almost the same failure probability as the bending geometries. It was clearly shown that this is not because the stress states in these geometries are equivalent, but because the wide plate geometry has two crack tips, which compensates the lower constraint level and resulting lower cleavage probability *per crack tip.*
- The present application of the clevage models is limited to situations where the amount of ductile tearing preceding final fracture by cleavage is limited to a small amount (0.2 mm). Beyond this, the finite element analysis used for the calculation of the Weibull stress values from which the cleavage fracture can be derived should account for the ductile tearing process.
- Although the predictions with the two- and three-parameter Weibull models are equivalent for intermediate cleavage probability ranges ($>10^{-2}$), they differ significantly for low probability values.
- A three-parameter model which incorporates a threshold value is considered to represent the physical reality better and is more suitable for predicting failure at lower probabilities.
- Before the three-parameter model becomes operational for actual safety assessment, a number of aspects of the model should be further explored. Sensitivity studies should be performed to reveal the influence of the threshold value on the probability predictions.
- All predictions in this investigation were based on two-dimensional finite element analyses with assumed plane strain behaviour. Although it is believed that the behaviour near the crack tip, which controls the cleavage predictions, is approximated well by assuming plane strain, three-dimensional analyses should be performed to verify this.

Acknowledgements

The work described in this report was carried out within the framework of the Dutch Collaborative Fracture Research Programme, which is co-ordinated by the Netherlands Welding Institute (NIL) and partly funded by the Netherlands Ministry of Economical Affairs. This financial support is gratefully acknowledged.

The experiments carried out for this investigation were prepared and performed by Hans Looy, (former) graduate student of the Plasticity and Fracture Section of the Laboratory for Materials Science and Technology of Delft University. His skill and dedication were much appreciated.

References

(1) VAN RONGEN, H. J. M. (1989) Proceedings of the 8th International Conference on Offshore Mechanics and Arctic Engineering (OMAE-8), (Edited by M. M. Salama *et al.*), *ASME*, New York, pp. 665–673.
(2) WALLIN, K., SAARIO, T., and TÖRRÖNEN, K. (1984) *Met. Sci.*, **18**, 13–16.
(3) BEREMIN, F. E. (1983) *Met. Trans*, **14A**, 2277–2287.
(4) WEIBULL, W. (1951) *ASME Applied Mechanics Division*, paper **51-A6**, pp. 293–297.
(5) BRIDGEMAN, P. W. (1952) *Studies in Large Plastic Flow and Fracture*, McGraw Hill, New York.
(6) KOERS, R. W. J., BRAAM, H., and BAKKER, A. (1989) *Advances in fracture research* (*ICF7*), (Edited by K. Salama *et al.*), Pergamon, Oxford, pp. 379–389.
(7) DEDOVIC, S., BAKKER, A., and LATZKO, D. G. H. (1988) *Int. J. Fatigue Fracture Engng Mater. Structures*, **11**, 251–266.